

Published in final edited form as:

Nat Microbiol. 2019 January ; 4(1): 62–70. doi:10.1038/s41564-018-0280-x.

Pneumolysin binds to the Mannose-Receptor C type 1 (MRC-1) leading to anti-inflammatory responses and enhanced pneumococcal survival

Karthik Subramanian^{1,#}, Daniel R Neill^{2,#}, Hesham Malak^{2,§}, Laura Spelmink^{1,§}, Shadia Khandaker², Giorgia Dalla Libera Marchiori¹, Emma Dearing², Alun Kirby³, Marie Yang², Adnane Achour⁴, Johan Nilvebrant⁵, Per-Åke Nygren⁵, Laura Plant¹, Aras Kadioglu^{2,*;¶}, and Birgitta Henriques-Normark^{1,6,7,*;¶}

¹Department of Microbiology, Tumor and Cell Biology, Karolinska Institutet, SE-171 77 Stockholm, Sweden

²Institute of Infection and Global Health, Ronald Ross Building, 8 West Derby Street, University of Liverpool, Liverpool, UK

³Centre for Immunology and Infection, Department of Biology and Hull York Medical School, University of York, York, UK

⁴Science for Life Laboratory, Department of Medicine Solna, Karolinska Institutet, and Department of Infectious Diseases, Karolinska University Hospital, Solna, Stockholm, SE, 17176, Sweden

⁵Division of Protein Technology, School of Biotechnology, Royal Institute of Technology (KTH), SE-106 91 Stockholm, Sweden

⁶Clinical Microbiology, Karolinska University Hospital, SE-171 76 Stockholm, Sweden

⁷Lee Kong Chian School of Medicine (LKC) and Singapore Centre on Environmental Life Sciences Engineering (SCELSE), Nanyang Technological University, Singapore 639798, Singapore

Users may view, print, copy, and download text and data-mine the content in such documents, for the purposes of academic research, subject always to the full Conditions of use:http://www.nature.com/authors/editorial_policies/license.html#terms

*Correspondence to Prof. Birgitta Henriques-Normark (birgitta.henriques@ki.se) and Prof. Aras Kadioglu (a.kadioglu@liverpool.ac.uk).

#Co-first authors

¶Co-senior authors

§These authors contributed equally

Life Sciences Reporting Summary

Further information on experimental design is available in the Life Sciences Reporting Summary.

Data availability

The data that support the findings of this study are available from the corresponding authors upon reasonable request.

Author contributions

K.S., D.R.N., L.S., A.K. and B.H.N. designed the study. K.S., L.S., G.D.M., H.M., S.K., E.D., M.Y., D.R.N., A.A., J.N., P.N. and L.P. performed experiments. K.S., L.S., D.R.N., A.K. and B.H.N. wrote the manuscript, and the other authors contributed to writing. All authors read and approved the final version of the manuscript.

Competing interests

The authors declare that no competing interests exist.

Abstract

Streptococcus pneumoniae (the pneumococcus) is a major cause of mortality and morbidity globally, and the leading cause of death in under-five year olds. The pneumococcal cytolysin pneumolysin (PLY) is a major virulence determinant, known to induce pore-dependent pro-inflammatory responses. These inflammatory responses are driven by PLY-host cell membrane cholesterol interactions, with binding to a host cell receptor not previously demonstrated. However, here we discovered a receptor for PLY, whereby pro-inflammatory cytokine responses and TLR signaling are inhibited upon PLY binding to the Mannose-Receptor C type 1 (MRC-1) in human dendritic cells (DCs) and murine alveolar macrophages, along with upregulation of the cytokine suppressor SOCS1. Moreover, PLY-MRC-1 interaction mediates pneumococcal internalization into non-lysosomal compartments and polarizes naive T cells into an IFN- γ ^{low}, IL-4^{high} and FoxP3⁺ immunoregulatory phenotype. In mice, PLY-expressing pneumococci co-localize with MRC-1 in alveolar macrophages, and induce lower pro-inflammatory cytokine responses and reduced neutrophil infiltration, compared to a PLY-mutant. *In vivo*, MRC-1-inhibition using blocking antibodies or MRC-1 deficient mice, show reduced bacterial loads in the airways. In conclusion, we show that pneumococci use PLY-MRC-1 interactions to downregulate inflammation and enhance bacterial survival in the airways. This has important implications for future vaccine design.

Streptococcus pneumoniae is a common colonizer of the upper respiratory tract of healthy children, but also a major cause of life-threatening diseases such as pneumonia, septicaemia and meningitis, resulting in death of over 800,000 children annually¹. The cholesterol-binding pore-forming toxin pneumolysin (PLY) is expressed by most disease-causing isolates and is required for virulence^{2,3} and host-to-host transmission⁴. PLY is a multi-functional protein, which at sublytic doses can activate complement⁵, re-arrange cytoskeleton of host cells⁶, and induce pro-inflammatory cytokine responses⁷. PLY is released during bacterial autolysis, but has also been shown to be localized on the pneumococcal cell wall, thereby accessible to extracellular proteases⁸. The surface localization of PLY allows for speculation of a non-cholesterol receptor on host cells.

Alveolar macrophages and dendritic cells (DCs) are the major resident immune cells in alveoli and mediate protection from pathogens. The mannose receptor, MRC-1 (CD206), is a M2 phenotype marker⁹ and a phagocytic receptor¹⁰ that is mostly expressed by tissue macrophages, including alveolar macrophages¹¹. MRC-1 binds to endogenous and microbial antigens such as capsular polysaccharides^{12,13}. Furthermore, studies have demonstrated that MRC-1 influences pneumococcal uptake by Schwann and olfactory cells, but they did not show co-localization^{14,15}. It is not clear which macrophage receptors recognize pneumococci in the nasopharynx and lungs and what bacterial properties interacts with the receptors mediating pneumococcal uptake. Here, we discovered a role for PLY in driving anti-inflammatory responses and lysosomal escape in macrophages and DCs by directly binding to MRC-1, thereby promoting pneumococcal internalization and survival in the host.

We first compared the cytokine response induced by PLY by infecting different immune cells, primary human monocyte-derived dendritic cells (DCs), neutrophils and THP-1

monocyte-derived macrophages, with a low dose (MOI of 1) of the pneumococcal strain T4R (expressing PLY), or its isogenic PLY mutant T4R *ply*. The non-encapsulated strain T4R (isogenic capsular mutant of the encapsulated serotype 4 strain T4) was used for the *in vitro* experiments to increase bacterial uptake since the capsule impedes bacterial adhesion to host cells¹⁶. We found lower secretion of the pro-inflammatory cytokines TNF- α , IL-1 β and IL-12 from DCs challenged with PLY-proficient T4R compared to the mutant T4R *ply*, which was in contrast to THP-1-derived macrophages and neutrophils (Fig.1a, Supplementary Fig.1a-b). This PLY-dependent inhibition of cytokine responses was also observed using the encapsulated strains T4 and T4 *ply* (Fig.1b). The cytokine inhibition was independent of cell death as determined by measuring LDH release (Supplementary Fig. 1c), but dependent on bacterial uptake since secretion of TNF- α was reduced by blocking phagocytosis using cytochalasin D and wortmannin (Supplementary Fig.1d). Treatment with cytochalasin D, an inhibitor of actin polymerization, inhibited cytokine production by DCs and THP-1 macrophages in a PLY-independent manner. Pre-treatment with purified endotoxin-free PLY at 100 ng/ml inhibited IL-12 production by ~50% from DCs infected with T4R *ply* in a dose-dependent manner, independent of cell death (Supplementary Fig. 1e). To study strain dependency and the influence of the challenge dose we then infected DCs, THP-1 macrophages, neutrophils and bone-marrow derived macrophages (BMDMs) with the pneumococcal strains D39 of serotype 2, or its isogenic PLY mutant, D39 *ply*, at different MOIs and measured IL-1 β release and cell death (Supplementary Fig.1f-i). We observed that at lower infection doses (MOI of 0.1 or 1), the mutant D39 *ply* induced higher levels of IL-1 β in DCs and BMDMs (but not in neutrophils and THP-1 macrophages), independent of cell death. However, at MOI of 10, the pattern was reversed and wild-type D39 induced higher IL-1 β release, but this was also accompanied by ~2 fold higher cell death.

We then performed a TLR signalling q-PCR array using RNA from DCs infected for 9hrs with T4R or T4R *ply*. Expression of all genes, except IFN β 1, was upregulated following infection with T4R *ply* compared to T4R infected cells (Supplementary Fig.1j), indicating that PLY-expression has a general inhibitory effect on cytokine induction and inflammatory signalling in DCs.

To explore mechanisms behind this inhibitory effect of PLY on DCs, we measured expression of the negative regulators of NF- κ B, AP-1 and STAT1 pro-inflammatory signalling pathways. We identified upregulation of Suppressor of Cytokine Signalling 1, SOCS117, mRNA in DCs infected with T4R, but not with T4R *ply* (Fig.1c). Kinetic analysis revealed that SOCS1 mRNA increased 6hrs post infection (pi) and peaked at 9hrs (Supplementary Fig.1k). Concurrent with mRNA, protein levels of SOCS1 were higher in DCs at 9hrs pi with T4R compared to T4R *ply* (Fig.1d). However, SOCS1 expression remained unaffected in THP-1 macrophages, (Supplementary Fig.1l), confirming the cell-type specific effect.

Since SOCS1 is a known inhibitor of STAT signalling¹⁸, we measured phosphorylated STAT1 and found delayed phosphorylation in T4R-infected DCs as compared to T4R *ply* (Fig.1e). Pre-treatment with the STAT inhibitor stattic inhibited secretion of TNF- α , IL-1 β and IL-12 (Supplementary Fig.1m-o). Besides STAT1, we also found lower levels of NF- κ B

in T4R-infected DCs compared to T4R *ply* (Fig.1f). Together, our data suggest that PLY-expression inhibits pro-inflammatory signalling via STAT1 and NF- κ B in DCs, possibly via induction of the cytokine suppressor, SOCS1.

To identify the host receptor interacting with PLY, we performed a pull-down assay using purified PLY. We identified 32 proteins exclusively from DC lysates of which three were surface proteins, Integrin alpha-M, Mannose Receptor C type 1 (MRC-1), and Galectin-1 (Supplementary Table 1). We further investigated the lectin receptor MRC-1, since it has previously been reported to have immunosuppressive properties¹⁹. To confirm the interaction between MRC-1 and PLY, we performed immunoprecipitation of MRC-1 from native DC lysates using anti-PLY coupled beads (Supplementary Fig.2a). To assess whether MRC-1 binding to PLY was mediated via glycan recognition, we performed enzymatic deglycosylation of PLY to remove bound glycans as evident by slightly higher electrophoretic gel mobility (Supplementary Fig.2b). Importantly, MRC-1 co-immunoprecipitated with both native and deglycosylated PLY from native DC lysates (Supplementary Fig.2c). We found that MRC-1 was selectively expressed by DCs and M-CSF derived macrophages (M2 polarized), but not by THP-1, neutrophils or GM-CSF derived macrophages (M1 polarized) (Supplementary Fig.2d-e). Interestingly, DCs upregulated MRC-1 expression upon infection with T4R, compared to T4R *ply* (Supplementary Fig.2f). Similar to human DCs, BMDMs isolated from wild-type, but not MRC-1^{-/-} mice, upregulated the MRC-1 protein upon infection with strain D39 as compared to its isogenic PLY-deficient mutant, D39 *ply* (Supplementary Fig.2g). The capsular mutant (D39 *cps*) induced lower upregulation of MRC-1 than D39 (Supplementary Fig.2h). Analysis of MRC-1 expression at different MOIs revealed that DCs and BMDMs upregulated MRC-1 in a dose-dependent way in response to D39, as compared to D39 *ply*, and the difference was significant at MOI of 1 (Supplementary Fig.2i-1). Neutrophils and THP-1 macrophages showed very low MRC-1 expression that did not change significantly upon infection. Surface plasmon resonance analysis confirmed the PLY-MRC-1 interaction showing a K_D value of 4.5×10^{-8} M (Fig.2a). The interaction was also verified in the reverse orientation (Supplementary Fig.2m), and the specificity was shown using control proteins (Supplementary Fig.2n). To study the specific interaction of MRC-1 with PLY versus capsular polysaccharides, we performed ELISA to measure binding of immobilized MRC-1 with PLY dose-dependently in the presence or absence of purified serotype 2 or 4 capsules. We found that MRC-1 binds to the type 2, but not the type 4 capsule (Supplementary Fig. 2o). Importantly, MRC1 still binds to PLY even in the presence of capsule although to lesser extent (Supplementary Fig.2o). To identify the region of interaction, we performed a solid-phase binding assay using purified PLY domains and an Fc-construct containing the mannose-binding C-type lectin-like carbohydrate recognition domains of MRC-1 (CTLD4-7-Fc). We found that domain 4 of PLY is key to MRC-1-PLY-interaction as purified domain 4, but not domains 1-3, bound the CTLD4-7-Fc construct (Fig. 2b). The non-pore-forming PLY mutant (PdB)²⁰ showed reduced binding compared to cytolytic PLY (Fig.2b), indicating that active PLY is required for MRC-1 binding.

Next, we investigated the localization patterns of MRC-1 and PLY in DCs using immunofluorescence microscopy. Wild-type DCs or MRC-1-deficient DCs (treated with MRC-1 siRNA), were incubated for 45 min with recombinant active PLY. PLY co-localized

with MRC-1 and the early endosomal antigen EEA-1, indicating uptake by DCs (Fig.2c). In contrast, PLY-binding was reduced in MRC-1-deficient DCs. In addition, the non-poreforming PLY mutant (PdB) did not co-localize with MRC-1 (Fig.2c). At 90 min post pneumococcal challenge, internalized T4R co-localized with MRC-1, but did not co-localize with lysosomes, while the converse was observed for T4R *ply* (Fig.2d). To test whether bacterial internalization via MRC-1 inhibits fusion of pneumococcal-infected vacuoles with lysosomes, we used antibody-opsonized pneumococci as a control to engage Fc gamma receptor-mediated phagocytosis²¹. Strikingly, opsonized T4 did not co-localize with MRC-1 and co-stained with lysosomes in contrast to the non-opsonized control (Supplementary Fig. 2p). Moreover, opsonized T4 elicited similar levels of TNF- α and IL-1 β from DCs as T4 *ply* (Supplementary Fig.2q). To explore whether active PLY is required for interaction with MRC-1 in clinical pneumococcal isolates, we used a serotype 1 strain expressing non-haemolytic PLY (BHN31 of ST306) and the clonally related haemolytic strain (BHN32 of ST228)²². We found that the non-haemolytic strain did not co-localize with MRC-1, but co-stained for lysosomes (Supplementary Fig.2r), and elicited higher cytokine production from DCs (Supplementary Fig.2s) as compared to the haemolytic strain. Together, our data suggest that pneumococcal internalization, due to interaction between active PLY and MRC-1, inhibits fusion of vacuoles containing pneumococci with lysosomes. This is supported by previous findings that MRC-1 regulates phagosomal trafficking following phagocytosis and limits fusion with lysosomes^{10,23}.

Furthermore, we found that uptake of PLY-proficient T4R, but not T4R *ply*, was reduced by 50% in MRC-1 depleted DCs (Fig.3a and Supplementary Fig.3a). Also, depletion of MRC-1 in DCs led to significantly higher levels of IL-12, TNF- α and IL-6 upon T4R-infection (Fig. 3b), and abrogated SOCS1 expression (Supplementary Fig.3b). This suggests that activation of MRC-1 by PLY triggers upregulation of SOCS1 in DCs, thereby reducing secretion of inflammatory cytokines.

Since DCs are professional antigen-presenting cells, we investigated the role of MRC-1 in DC-primed CD4⁺ T-helper cell cytokine responses after pneumococcal challenge. We found that DCs depleted of MRC-1 using siRNA and infected with T4R (in contrast to T4R *ply*), elicited higher IFN- γ (Th1 cytokine) and lower IL-4 (Th2 cytokine) levels from naive T-helper cells in co-culture, compared to DCs treated with control siRNA (Fig.3c-d). A similar trend was observed in DCs stimulated with purified PLY. To further characterize the phenotype of T cells co-cultured with DCs, we measured FoxP3, a regulatory T cell marker²⁴ and found that DCs infected with T4R (but not with T4R *ply*) and those treated with purified PLY, induced higher FoxP3 expression in naive T helper cells upon co-culture (Fig.3e, Supplementary Fig.3c). FoxP3 upregulation in T cells was abolished when co-cultured with DCs treated with MRC-1 siRNA. Similar to human DCs, murine BMDMs from WT mice that were infected with D39 (in contrast to D39 *ply*) and co-cultured with CD4⁺ murine T cells, resulted in higher regulatory (FoxP3, IL-10 expressing) T cells and lower Th1 cells (T-bet, IFN- γ expressing) as compared to BMDMs from MRC-1^{-/-} mice (Fig.3f, Supplementary Figs. 3d-f). Our data are in agreement with earlier findings showing that MRC-1 expression in DCs inhibits CD45 and induces T-cell tolerance²⁵, and that PLY is required for robust regulatory T cell induction *in vivo*²⁶.

To verify our findings *in vivo*, we challenged wild-type C57BL/6J mice intranasally with 10^6 CFU of wild-type T4 or the mutant T4 *ply*. At 6hrs post infection (pi), bronchoalveolar lavage fluids (BALF) were collected and lung alveolar macrophages isolated. We observed intracellular co-localization of strain T4 with MRC-1, but not with lysosomes (Fig.4a). In contrast, intracellular T4 *ply* did not co-localize with MRC-1, but co-stained with lysosomes (Fig.4a, Supplementary Fig.4a). *Ex vivo*, murine alveolar macrophages secreted lower levels of pro-inflammatory cytokines upon infection with T4R compared to T4R *ply*. This difference was reduced by pre-treatment with anti-MRC-1 (Supplementary Fig.4b-c). In agreement with these results, T4 *ply* infected mice had higher levels of pro-inflammatory cytokines, TNF- α , IL-12 and IL-1 β , and lower levels of anti-inflammatory cytokines, IL-10 and TGF- β , in the BALF, compared to mice infected with T4 (Fig.4b, Supplementary Fig. 4d). In addition, T4 *ply* infected mice had higher numbers of neutrophils and monocytes in the BALF (Supplementary Fig.4e). The enhanced inflammation and higher infiltration of phagocytes were concurrent with the higher clearance of T4 *ply* compared to T4 from the airways of infected mice (Fig.4c). Mice pre-treated with antibodies to block MRC-1 prior to infection with T4 had significantly higher levels of TNF- α and IL-12, and lower levels of IL-10 in BALF at 6hrs pi as compared to isotype antibody-treated controls (Fig.4d, Supplementary Fig.4f). Anti-MRC-1 treated mice had 50% lower bacterial counts in the lower airways compared to controls (Fig.4e), and intracellular bacteria did not co-localize with MRC-1 in alveolar macrophages (Supplementary Fig.4g). Importantly, MRC-1^{-/-} mice also had significantly decreased bacterial numbers in the nasopharynx at 7 and 14 days post challenge compared to wild-type mice in a pneumococcal carriage model with strain D39 (Fig.4f). In wild-type mice, MRC-1⁺ macrophages were found to rapidly accumulate in the nasopharynx following pneumococcal colonization (Supplementary Fig.5a-b). Similar to anti-MRC-1 treated mice, MRC-1^{-/-} mice had higher levels of pro-inflammatory cytokines, TNF- α and IL-6, and lower levels of anti-inflammatory IL-10 and TGF- β in the nasopharynx compared to WT mice at 6hrs and 1 day pi (Supplementary Fig.5c-f).

MRC-1 mediated phagocytosis is of particular significance in the lungs, as MRC-1 is abundantly expressed by alveolar macrophages. A previous study by Dorrington et al. highlighted the crucial role of the scavenger receptor MARCO in anti-pneumococcal immunity in the nasopharynx and suggested a minimal role for MRC-127. However, the authors in that study used a 100-fold higher infection dose (1×10^7 CFU) for colonization compared to our study and we have previously shown that in contrast to high-density infection, low density pneumococcal carriage induces immunoregulatory responses characterized by sustained elevation of nasopharyngeal TGF- β 1, regulatory T cells and MRC-1 expressing macrophages²⁶. In the current study, we demonstrate that the infection dose determines the nature of cytokine response to PLY, where lower infection doses eliciting cytokine inhibition. Hence, our results suggest that the infection dose is critical when studying host responses to pneumococcal infections.

PLY is not a typical adhesin and has previously been considered to be cytosolic and released only upon bacterial lysis. However, recent data using transmission electron microscopy²⁸ show that pneumolysin can be surface localized, suggesting that it can be available for interactions with host receptors. The above data support our discovery that PLY interacts with MRC-1 which is a finding that represents a conceptual change in our current

understanding. Our results suggest that MRC-1-PLY interaction is not mediated by glycan recognition, since MRC-1 also binds to deglycosylated PLY, and the interaction is specifically mediated by C type lectin domains 4-7 of MRC-1 and domain 4 of PLY.

In conclusion, we discovered a significant role for PLY, whereby MRC-1 acts as a receptor for PLY, enabling pneumococci to invade MRC-1 proficient immune cells including DCs and alveolar macrophages in the airways, thereby dampening cytokine responses to establish intracellular residency of pneumococci. Whilst MRC-1 has previously been demonstrated to bind pneumococcal capsular polysaccharides^{12,13}, we show here that it can also directly bind to PLY. This is a hitherto unknown survival mechanism for the pneumococcus and has important implications for future vaccine design against infection. The potential mechanisms involved are summarized in Fig.4g.

Methods

Pneumococcal strains used

The encapsulated *S. pneumoniae* serotype 4 strain TIGR4 (T4; ATCC BAA-334) as well as its non-encapsulated isogenic mutant, T4R, and their isogenic PLY-deficient mutants T4 *ply* and T4R *ply* were used in this study. Clinical isolates of serotype 1 pneumococci expressing non-hemolytic PLY (BHN31 of ST306) or clonally related strain expressing haemolytic PLY, (BHN32 of ST228) were also used²². Bacteria were grown on blood agar plates at 37°C and 5% CO₂ overnight. Colonies were inoculated into C+Y medium and grown until exponential phase (OD₆₂₀ = 0.5). For opsonisation, pneumococci were incubated with 5% Type 4 anti-serum for 30 min at 37°C (Statens Serum Institut).

S. pneumoniae serotype 2, strain D39 (NCTC 7466), was obtained from the National Collection of Type Culture, London, UK. The pneumolysin-deletion D39 mutant D39 *ply* was kindly provided by Prof. Tim Mitchell (University of Birmingham). Capsular-deficient D39-J (D39 *cps*) and the double mutant in PLY and the capsule DKO (double knockout) (D39 *cps ply*) were kindly provided by Dr. Lucy Hathaway (University of Bern). D39 was cultured on blood agar base with 5% v/v horse blood, or in brain heart infusion broth (BHI; Oxoid, Basingstoke, UK) with 20% v/v FBS (Sigma), supplemented with 20 mg/ml spectinomycin (Sigma) for DKO.

Pneumolysin (PLY)

Recombinant PLY, mutant (PdB) or PLY domains (D1-3, D4), were expressed in *E. coli* and purified as previously described⁷. PLY D1-3 and D4 were kindly provided by Prof. Tim Mitchell (University of Birmingham). Haemolytic activity of PLY was 100,000 HU/mg. Purified toxin was passed six times through an endotoxin removal column (Profos AG, Germany) and absence of detectable LPS was confirmed with PyroGene Recombinant Factor C assay (Lonza; detection limit 0.01 EU/ml).

Cell isolation from buffy coats, cell-culture and infection

Monocytes were purified from buffy coats of healthy donors (Karolinska University Hospital and Uppsala University Hospital) using the RosetteSep™ monocyte purification kit (Stem

Cell Technologies) and Ficoll-Paque Plus (GE Healthcare) gradient centrifugation. For differentiation into DCs, monocytes were cultured in R10 (RPMI 1640, 2 mM L-glutamine, 10% FBS) supplemented with GM-CSF (40 ng/ml) and IL-4 (40 ng/ml) from Peprotech for 6 days. DCs were verified by flow cytometry to be >90% CD1a⁺ CD11c⁺. In co-culture experiments, at 24 hrs post infection, DCs were washed and incubated with naïve CD4⁺ T cells in a 1:10 ratio (DC: T cells) at 37°C. Supernatants were collected 5 days later for cytokine measurements by ELISA. Cytokine values were subtracted from control wells containing DCs alone. For infection, DCs were incubated with pneumococci at a multiplicity of infection (MOI) of 1 and extracellular bacteria were killed with 200 µg/ml gentamicin after 2 hrs of infection. Cytochalasin D (0.5 mM), wortmannin (0.1 mM) (Sigma) or stattic (5 µM) (Tocris Biosciences) were added to cells 15 min prior to pneumococcal infection. In some experiments, DCs were incubated with endotoxin-free PLY at 0.2 µg/ml diluted in R10 medium.

Human monocytic leukemia THP-1 cells (ATCC TIB-202) were cultivated in R10. For differentiation into macrophages, THP-1 cells were treated for 48 hrs with 20 ng/ml of phorbol myristate acetate (PMA) (Sigma).

Neutrophils were isolated from whole blood upon lysis of RBCs and enriched using the EasySep human neutrophil enrichment kit (StemCell Technologies) according to the manufacturer's instructions. Purified neutrophils were verified to be ~99% CD66b⁺CD16⁺. Human naïve T cells were purified from fresh PBMCs using the EasySep™ Human Naïve CD4⁺ T Cell Isolation Kit (Stem cell Technologies) and were verified by flow cytometry to be >95% CD3⁺CD4⁺. All cells used in this study were mycoplasma tested.

Isolation of mouse bone-marrow derived macrophage (BMDM) and culture

Bone-marrow cells were flushed from murine femurs and tibia. Macrophages were grown from bone marrow cells in Dulbecco's Modified Eagle's Medium (Sigma, UK) 10% v/v foetal calf serum (FCS; Sigma), 100 U/ml penicillin, 100 mg/ml streptomycin, and 100 mM L-glutamine (Sigma) supplemented with 20 ng/ml macrophage colony-stimulating factor (M-CSF; R&D systems). Cultures were maintained in a humidified atmosphere (5% CO₂) at 37°C, and medium was replaced on days 3 and 6. On day 6, cells were plated for use in assays. 6.25x10⁵ BMDM were cultured alone (untreated) or infected with D39, D39 *ply*, D39 *cps* or DKO (D39 *cps ply*)(1 macrophage: 10 bacteria) or stimulated with purified PLY (4 µg/ml). After 24 hrs incubation, supernatants were collected and used to assess cytokine production by ELISA or determine density of infection by Miles and Misra dilution.

BMDM-T cell co-culture

Naïve CD25⁻CD4⁺ T cells were purified from spleen of C57BL/6 or MRC-1^{-/-} mice by negative selection (Miltenyi Biotec). Non-CD4⁺ T cells and CD44⁺ memory T cells were labelled with biotinylated antibodies, before addition of anti-biotin microbeads and magnetic separation. CD4⁺ T-cell purity was >90%. Purified T-cells were added to 24 hrs pneumococcal stimulated BMDM at a ratio of 15:1 for 5 days. Culture supernatants were collected for ELISA and cells were stained for flow cytometry.

Cell viability assays

Cytotoxicity was determined in the culture supernatants by measuring the release of the enzyme lactate dehydrogenase (LDH) compared to a 100% lysis control using the Cytotoxicity kit (Roche) according to manufacturer's instructions.

Real time quantitative PCR (qPCR)

Total cellular RNA was extracted from cells using the RNeasy Kit (Qiagen). The concentration and purity of isolated RNA was determined spectrophotometrically with the Nanodrop ND 1000. cDNA was synthesized from the isolated RNA using the High Capacity cDNA Reverse Transcription kit (Applied Biosystems). The qPCR was performed using the iTaq Universal SYBR Green Supermix (BioRad) according to manufacturer's instructions. The following primers were used: Hs_SOCS1_1_SG, Hs_MRC1_1_SG and Hs_GAPDH_1_SG. Each primer pair was validated for specificity by performing melt curve analysis of the PCR product to ensure the absence of primer dimers and unspecific products. The mRNA expression level was normalized to the level of GAPDH and relative expression was determined with the 2^{-CT} method. The TLR Signaling qPCR array (Qiagen) was performed according to the manufacturer's instructions and analysed with the GeneGlobe Data analysis Center (Qiagen).

Mouse experiments and isolation of alveolar macrophages

All mice experiments were performed in accordance with the local ethical committee (Stockholms Norra djurförsöksetiska nämnd). Six- to seven- weeks old male wild-type C57BL/6J were used. Experiments with MRC-1^{-/-} mice were done at the University of Liverpool with the approval of the UK Home Office and the University of Liverpool ethics committee. MRC-1^{-/-} mice²⁹ were generated on a mixed 129SvJ and C57BL/6 background, and then backcrossed to C57BL/6 strain for at least 7 generations. Homozygous knockout mice were bred and maintained at the University of Nottingham and were a generous gift of Dr. Luisa Martinez-Pomares (University of Nottingham). WT and MRC-1^{-/-} mice used for infection were sex and age matched and no more than 12 weeks of age at the start of the experiment. WT and MRC-1^{-/-} mice were randomised independently to time points by technical staff with no role in study design. Researchers were blinded to the experimental group until the data analysis stage. Sample size calculations were determined to give 90% power, alpha = 5%, assuming expected mean CFU for WT of 1000 CFU/ml and S.D. of 5% (determined from previous studies). The experiments were powered to detect an expected difference between groups of 10%.

Pneumococcal nasopharyngeal carriage model

For induction of pneumococcal nasopharyngeal carriage, mice were lightly anaesthetized and 10 μ l PBS containing 1×10^5 CFU D39 was administered into the nostrils. The dose was confirmed by viable count following infection. At pre-chosen time intervals following infection, mice were sacrificed and nasopharynx, draining cervical lymph nodes and lungs were collected, passed through a 30 μ m cell strainer or homogenized with an Ultra-Turrax T8 homogeniser (IKA, Germany). Bacterial counts were determined from tissue homogenates by viable count on blood agar plates.

Invasive pneumococcal disease model

Mice were sedated by inhalation of 4% isofluorane and 50 μ l PBS containing 10^6 CFU of wild-type T4 or the PLY mutant, T4 *ply* was administered into the nostrils. To block MRC-1, 20 μ l of 0.1 mg/mL monoclonal anti-MRC-1 (Abcam) or isotype matched control (Abcam) was administered intranasally 30 min before infection. Post sacrifice, the lungs were perfused twice with ice-cold PBS containing 1 mM EDTA to collect the bronchoalveolar lavage fluid (BALF). To determine viable bacterial counts, serial dilutions of BALF were plated on blood agar plates followed by colony counting. Aliquots of BALF were frozen at -80°C for cytokine quantification by ELISA. To isolate alveolar macrophages, BALF was spun down at 400 g for 7 min at 4°C , resuspended in R10 medium (RPMI 1640 containing 2 mM L-glutamine and 10% foetal bovine serum (FBS)) and plated on coverslips for 1 hr to allow cells to attach. Unattached cells were removed by washes with PBS. Macrophages were verified phenotypically by flow cytometry (CD11c⁺ Siglec F⁺). The percentage of neutrophils (CD11b^{hi} Ly6G^{hi}) and monocytes (CD11b^{hi} Ly6C^{hi}) in the BALF was quantified by flow cytometry upon gating for viable cells stained using fixable viable dye eFluor 780 (Thermo Fisher Scientific).

MRC-1 knockdown using siRNA

DCs (6×10^6) were electroporated with 5 μ M siRNA from Life Technologies against MRC-1 (s53926, s53927, s53928) or scrambled control siRNA (4390843, 4390846) on day 4 of DC differentiation. The cells were electroporated with the Bio-Rad gene pulser (square wave, 500V, 0.5 ms with a single impulse) and immediately resuspended in fresh R10 medium. The cells were used 48 hrs post siRNA electroporation. Treatment with siRNA reduced MRC-1 protein expression by ~80% as evaluated by western blotting (Fig. S3A).

Flow Cytometry

Cells were fixed with 4 % PFA and stained with a mouse anti-MRC-1 (Abcam) and a goat-anti mouse Alexa Fluor 488 secondary antibody (Life Technologies). For intracellular staining, cells were fixed with 4% PFA and permeabilized with ice cold methanol. Cells were stained with phospho-STAT1 (Tyr 701) Alexa Fluor 488 conjugated rabbit antibody (Cell Signalling), rabbit anti-SOCS1 (ab135718) and assessed by flow cytometry using the Gallios Flow Cytometer. In addition, the following antibodies from Biolegend were used in this study : CD3 (100235), CD4 (100405), CD8a (100707), CD11b (101207), CD19 (152403), CD45 (103111), CD69 (104507), CD115 (135523), CD206 (MRC-1) (141707), F4/80 (123107), FOXP3 (126403), GATA3 (653805), Gr-1 (108411), MARCO (BioRad ED31), ROR γ t (654301), T-bet (644809). Antibodies were conjugated to fluorescein isothiocyanate (FITC), phycoerythrin (PE), PE-Cy7 or allophycocyanin (APC) and appropriate isotype controls were included in all experiments.

Quantification of cytokines

For cytokine measurement, cell-free culture supernatants were harvested 18 hrs pi and frozen at -20°C . The levels of human TNF- α , IL-12p70, IL-1 β , IFN- γ and IL-4, using the OptEIA™ ELISA kit (BD Biosciences). The levels of mouse TNF- α , IL-12p70, IL-1 β ,

IL-10 and TGF- β in the mouse BALF was measured using the respective mouse ELISA kits (BD Biosciences).

Enzymatic deglycosylation of PLY

PLY was deglycosylated under native conditions using the Protein Deglycosylation kit (Sigma) following the instructions of the kit. Briefly, 10 μ g of recombinant PLY was incubated with 1 μ l each of Peptide:N-glycosidase F, O-Glycosidase, Sialidase A, β -(1-4)-Galactosidase and β -N-acetylglucosaminidase in 50 μ l reaction buffer for 3 days at 37°C. The extent of deglycosylation was assessed by mobility shifts on SDS-PAGE gels.

Pull-down of PLY-interacting proteins and Co-IP with MRC-1

To identify proteins interacting with PLY, pull-down was performed on DC and THP-1 native cell lysates using recombinant PLY as the bait. Cells were lysed with native lysis buffer (Abcam) containing 1x protease inhibitors (Roche) on ice for 15 min. Briefly, lysate corresponding to 0.8 mg protein was precleared by incubating with Protein G-agarose beads (Pierce) for 30 min at 4°C. Subsequently, the precleared lysate was incubated with 1 μ g PLY (Cusabio) for 1 hr at 4°C and then incubated with Protein G beads conjugated to mouse anti-PLY (Abcam) with gentle rotation overnight at 4°C. As a control, lysates were incubated with isotype antibody or beads alone to distinguish non-specific interactions. The beads were washed thrice with PBS and the bound proteins were eluted by boiling in NuPAGE LDS sample buffer for 5 min at 95°C. The eluted proteins were identified using mass spectrometry at the Science for Life Laboratory in Uppsala, Sweden. The protein identifications were based on at least two matching peptides of 95% confidence per protein. To confirm the interaction between PLY and MRC-1, western blotting was performed on the eluate. MRC-1 was detected using rabbit anti-human MRC-1 (Abcam) and HRP-conjugated secondary goat anti-rabbit (GE Healthcare).

Surface plasmon resonance analysis

Surface plasmon resonance experiments were run on Biacore 3000 and T200 instruments (GE Healthcare) at 25°C with 10 mM HEPES Supplementaryemented with 2 mM CaCl₂ and 0.1 % (v/v) Tween 20 as running buffer. Pneumolysin (PLY; Causabio) and mannose receptor C type 1 (MRC-1; R&D Systems) were diluted to 10 μ g/mL in 10 mM NaOAc pH 4.5 and immobilized on CM5 chips by amine coupling to immobilization levels of 2200 and 12000 RU, respectively. PLY was buffer-exchanged into running buffer using a 3 kDa MWCO Amicon centrifugal filter device prior to injections. Human serum albumin was immobilized at 11000 RU in a separate flow cell as a negative control. Analytes were injected at 30 μ l/min and surfaces were regenerated using 10 mM HCl. Sensorgrams were double referenced using a blank flow cell and a buffer injection. Data for injections of PLY over MRC-1 were fitted to a Langmuir 1:1 interaction using BiaEval 4.1 software and the dissociation equilibrium constant was calculated from average association and dissociation rate constants obtained from three separate dilution series analyzed on two different sensor chips. Human serum albumin, bovine serum albumin and Trastuzumab (Herceptin®) were injected at 1 μ M as negative controls for non-specific binding. The influence of mannose on MRC-1 binding was evaluated by pre-incubating 100 nM of MRC with 0.5 mM D-mannose

or D-glucose (Sigma) for 1 hr in running buffer prior to injection of the mixed samples over the PLY immobilized chip.

ELISA to measure MRC-1-PLY binding

Briefly, 96-well flat-bottomed plates (Sigma, UK) were coated overnight with 1.25-10 µg/ml of mannose receptor, full-length (2534-MR-050) or truncated constructs CTLD4-7-Fc, CR-FNII-CTLD1-3-Fc30, a generous gift from Dr Luisa Martinez-Pomares (University of Nottingham, UK), in the presence or absence of galactose or mannose (Sigma, UK) in coating buffer (15 mM Na₂CO₃, 35 mM NaHCO₃, pH 9.6). Wells were blocked with 200 µl of 20% (v/v) FBS in PBS for 2 hrs, and then washed three times with 250 µl PBS, 0.05% (v/v) Tween 20 (Sigma, UK). 10 µg/ml of PLY, PdB, PLY domains 1-3 or PLY domain 4 was added and incubated at 37°C for 1 hr. Wells were washed again with PBS and bound proteins were detected using PLY polyclonal antibody (Abcam ab71811) in blocking buffer. Plates were incubated with anti-rabbit IgG alkaline phosphatase (Abcam ab6722) in blocking buffer. Bound antibodies were detected in using the chromogenic substrate p-nitrophenylphosphate (pNPP) for 30 min. 1M NaOH was added to all wells and the absorbance was measured at 405 nm.

To study the specific interaction of MRC-1 with PLY versus capsular polysaccharides, immobilized MRC1 was incubated with PLY (0-5 µg/ml) in the presence or absence of 2.5 µg/ml of purified serotype 2 or type 4 capsules (SSI Diagnostica). Bound PLY in the presence or absence of capsule was detected using mouse anti-PLY and anti-mouse IgG-HRP. Binding of purified capsule to MRC-1 was detected using rabbit anti-capsule and anti-rabbit IgG-HRP. Bound antibodies were detected using the chromogenic substrate, tetramethylbenzidine (TMB). 1M phosphoric acid was used as stop solution and absorbance was measured at 450 nm.

Immunofluorescence microscopy

Briefly, cells were fixed with 4% paraformaldehyde buffered in PBS for 10 min. Subsequently, the cells were permeabilized using PBS containing 0.5% Tween20 for 15 min. To block non-specific interactions, cells were incubated with 5% FBS in PBS for 1 hr. Lysosomes were stained using lysotracker deep red (Thermo Fisher Scientific) prior to fixation. Early endosomes were stained using Alexa 647 conjugated anti-EEA1 (Abcam). PLY was stained using mouse anti-PLY (Abcam) and Alexa488-goat anti-mouse secondary antibody (Thermo Fisher Scientific). MRC-1 was detected using rabbit anti-MRC-1 (Abcam) and Alexa 555-goat anti-rabbit secondary antibody (Thermo Fisher Scientific). Pneumococci were stained using rabbit anti-pneumococcal anti-serum (Eurogentec) labeled with Alexa 488 using Zenon rabbit IgG labeling kit (Thermo Fisher Scientific). Type 1 clinical strains were stained using anti-serum Type 1 (Statens Serum Institut). Samples were washed twice with PBS between the antibody incubations and mounted on slides using ProLong Diamond antifade reagent containing DAPI (Thermo Fisher Scientific). Images were acquired using the Delta Vision Elite microscope under the 100x objective (GE Healthcare).

Immunohistochemistry

Draining cervical lymph nodes were snap frozen in liquid nitrogen and 7 μm sections were cut. Staining was performed with fluorochrome conjugated MRC-1 (biotin 647, BD biosciences) and appropriate isotype matched controls. Sections were mounted in ProLong Gold (Invitrogen) and images were taken using a Zeiss Axioplan LSM 510 confocal microscope as single optical slices of between 0.8 and 1.0 μm . Images were analyzed using Zeiss LSM image browsing software v4.

Western blotting

Cells were lysed with RIPA buffer containing 1 \times protease inhibitors (Roche) on ice for 15 minutes. Cell debris and nuclear material were pelleted by centrifuging at 13000 rpm for 15 min. Lysate corresponding to 25 μg protein was boiled for 5 min at 95°C in NuPAGE LDS sample buffer and resolved on 4-12% Bis-Tris gel (Invitrogen). Proteins were transferred to polyvinylidene fluoride (PDVF) membrane and blocked with 5% skim milk powder in PBS containing 0.1% Tween-20. Proteins were detected using the following antibodies: mouse anti-human MRC-1 (Abcam), SOCS1 antibody, NF κ B(p65) antibody (Santa Cruz) and a phospho-I κ B α (Ser32) (Santa Cruz). Rabbit anti-GAPDH (Sigma) and Rabbit Histone H2A2.Z (Cell signaling Technologies) was used as a loading control. Anti-rabbit IgG or anti-mouse IgG conjugated to horseradish peroxidase (GE Healthcare) were used as secondary antibodies. Blots were developed with Amersham™ ECL Plus Western blotting detection system (GE Healthcare), using a ChemiDoc™ XRS+ (Bio-Rad Laboratories).

Statistical analysis

Data were statistically analysed using GraphPad Prism 5.04. Data of immune cells prepared from human donor blood were analysed with a Wilcoxon matched-pairs signed rank test. Data from THP-1 macrophages were analysed with a Mann Whitney test. Comparison between groups was done with a one-way or two-way ANOVA followed by a Bonferroni or Tukey's post-test as indicated. Normalized data was analysed with an unpaired t-test. Differences were considered significant at * $P < 0.05$, ** $P < 0.01$ and ns denotes not significant.

Supplementary Material

Refer to Web version on PubMed Central for supplementary material.

Acknowledgments

The work in Sweden was supported by grants from the Swedish Research Council, Stockholm County Council, the Swedish Foundation for Strategic Research (SSF), and the Knut and Alice Wallenberg foundation. The work in Liverpool was supported by funding from the UK Medical Research Council (Programme Grant MR/P011284/1), a Sir Henry Dale Fellowship (awarded to D.R.N.) and jointly funded by the Wellcome Trust and the Royal Society (Grant Number 204457/Z/16/Z), a British Commonwealth Scholarship (awarded to S.K.), Embassy of the Kingdom of Saudi Arabia Scholarship (awarded to H.M.) and the Institute of Infection & Global Health, University of Liverpool. We thank the Science for Life Laboratory Mass Spectrometry Based Proteomics Facility in Uppsala for the LC-MS analysis.

References

1. Black RE, et al. Global, regional, and national causes of child mortality in 2008: a systematic analysis. *Lancet*. 2010; 375:1969–1987. DOI: 10.1016/S0140-6736(10)60549-1 [PubMed: 20466419]
2. Berry AM, Yother J, Briles DE, Hansman D, Paton JC. Reduced virulence of a defined pneumolysin-negative mutant of *Streptococcus pneumoniae*. *Infection and immunity*. 1989; 57:2037–2042. [PubMed: 2731982]
3. Hirst RA, et al. *Streptococcus pneumoniae* deficient in pneumolysin or autolysin has reduced virulence in meningitis. *The Journal of infectious diseases*. 2008; 197:744–751. DOI: 10.1086/527322 [PubMed: 18260758]
4. Zafar MA, Wang Y, Hamaguchi S, Weiser JN. Host-to-Host Transmission of *Streptococcus pneumoniae* Is Driven by Its Inflammatory Toxin, Pneumolysin. *Cell Host Microbe*. 2017; 21:73–83. DOI: 10.1016/j.chom.2016.12.005 [PubMed: 28081446]
5. Paton JC, Rowan-Kelly B, Ferrante A. Activation of human complement by the pneumococcal toxin pneumolysin. *Infection and immunity*. 1984; 43:1085–1087. [PubMed: 6698602]
6. Iliev AI, Djannatian JR, Nau R, Mitchell TJ, Wouters FS. Cholesterol-dependent actin remodeling via RhoA and Rac1 activation by the *Streptococcus pneumoniae* toxin pneumolysin. *Proceedings of the National Academy of Sciences of the United States of America*. 2007; 104:2897–2902. DOI: 10.1073/pnas.0608213104 [PubMed: 17301241]
7. McNeela EA, et al. Pneumolysin activates the NLRP3 inflammasome and promotes proinflammatory cytokines independently of TLR4. *PLoS Pathog*. 2010; 6:e1001191. doi: 10.1371/journal.ppat.1001191 [PubMed: 21085613]
8. Price KE, Camilli A. Pneumolysin localizes to the cell wall of *Streptococcus pneumoniae*. *J Bacteriol*. 2009; 191:2163–2168. DOI: 10.1128/JB.01489-08 [PubMed: 19168620]
9. Gordon S. Alternative activation of macrophages. *Nature reviews. Immunology*. 2003; 3:23–35. DOI: 10.1038/nri978
10. Kang PB, et al. The human macrophage mannose receptor directs *Mycobacterium tuberculosis* lipoarabinomannan-mediated phagosome biogenesis. *J Exp Med*. 2005; 202:987–999. DOI: 10.1084/jem.20051239 [PubMed: 16203868]
11. Taylor PR, Gordon S, Martinez-Pomares L. The mannose receptor: linking homeostasis and immunity through sugar recognition. *Trends in immunology*. 2005; 26:104–110. DOI: 10.1016/j.it.2004.12.001 [PubMed: 15668126]
12. Zamze S, et al. Recognition of bacterial capsular polysaccharides and lipopolysaccharides by the macrophage mannose receptor. *The Journal of biological chemistry*. 2002; 277:41613–41623. DOI: 10.1074/jbc.M207057200 [PubMed: 12196537]
13. McGreal EP, et al. The carbohydrate-recognition domain of Dectin-2 is a C-type lectin with specificity for high mannose. *Glycobiology*. 2006; 16:422–430. DOI: 10.1093/glycob/cwj077 [PubMed: 16423983]
14. Macedo-Ramos H, et al. Evidence of involvement of the mannose receptor in the internalization of *Streptococcus pneumoniae* by Schwann cells. *BMC Microbiol*. 2014; 14:211. doi: 10.1186/s12866-014-0211-9 [PubMed: 25085553]
15. Macedo-Ramos H, et al. Olfactory ensheathing cells as putative host cells for *Streptococcus pneumoniae*: evidence of bacterial invasion via mannose receptor-mediated endocytosis. *Neurosci Res*. 2011; 69:308–313. DOI: 10.1016/j.neures.2010.12.015 [PubMed: 21192991]
16. Kadioglu A, Weiser JN, Paton JC, Andrew PW. The role of *Streptococcus pneumoniae* virulence factors in host respiratory colonization and disease. *Nat Rev Microbiol*. 2008; 6:288–301. DOI: 10.1038/nrmicro1871 [PubMed: 18340341]
17. Yoshimura A, Naka T, Kubo M. SOCS proteins, cytokine signalling and immune regulation. *Nat Rev Immunol*. 2007; 7:454–465. DOI: 10.1038/nri2093 [PubMed: 17525754]
18. Yasukawa H, Sasaki A, Yoshimura A. Negative regulation of cytokine signaling pathways. *Annu Rev Immunol*. 2000; 18:143–164. DOI: 10.1146/annurev.immunol.18.1.143 [PubMed: 10837055]

19. Chieppa M, et al. Cross-linking of the mannose receptor on monocyte-derived dendritic cells activates an anti-inflammatory immunosuppressive program. *J Immunol.* 2003; 171:4552–4560. [PubMed: 14568928]
20. Paton JC, et al. Purification and immunogenicity of genetically obtained pneumolysin toxoids and their conjugation to *Streptococcus pneumoniae* type 19F polysaccharide. *Infect Immun.* 1991; 59:2297–2304. [PubMed: 2050399]
21. Guilliams M, Bruhns P, Saeys Y, Hammad H, Lambrecht BN. The function of Fcγ receptors in dendritic cells and macrophages. *Nat Rev Immunol.* 2014; 14:94–108. DOI: 10.1038/nri3582 [PubMed: 24445665]
22. Littmann M, et al. *Streptococcus pneumoniae* evades human dendritic cell surveillance by pneumolysin expression. *EMBO Mol Med.* 2009; 1:211–222. DOI: 10.1002/emmm.200900025 [PubMed: 20049723]
23. Rajaram MVS, et al. M. tuberculosis-Initiated Human Mannose Receptor Signaling Regulates Macrophage Recognition and Vesicle Trafficking by Fcγ-Chain, Grb2, and SHP-1. *Cell Rep.* 2017; 21:126–140. DOI: 10.1016/j.celrep.2017.09.034 [PubMed: 28978467]
24. Sakaguchi S, Miyara M, Costantino CM, Hafler DA. FOXP3+ regulatory T cells in the human immune system. *Nat Rev Immunol.* 2010; 10:490–500. DOI: 10.1038/nri2785 [PubMed: 20559327]
25. Schuette V, et al. Mannose receptor induces T-cell tolerance via inhibition of CD45 and up-regulation of CTLA-4. *Proc Natl Acad Sci U S A.* 2016; 113:10649–10654. DOI: 10.1073/pnas.1605885113 [PubMed: 27601670]
26. Neill DR, et al. Density and duration of pneumococcal carriage is maintained by transforming growth factor beta1 and T regulatory cells. *Am J Respir Crit Care Med.* 2014; 189:1250–1259. DOI: 10.1164/rccm.201401-0128OC [PubMed: 24749506]
27. Dorrington MG, et al. MARCO is required for TLR2- and Nod2-mediated responses to *Streptococcus pneumoniae* and clearance of pneumococcal colonization in the murine nasopharynx. *J Immunol.* 2013; 190:250–258. DOI: 10.4049/jimmunol.1202113 [PubMed: 23197261]
28. Shak JR, et al. Novel role for the *Streptococcus pneumoniae* toxin pneumolysin in the assembly of biofilms. *mBio.* 2013; 4doi: 10.1128/mBio.00655-13
29. McKenzie EJ, et al. Mannose receptor expression and function define a new population of murine dendritic cells. *J Immunol.* 2007; 178:4975–4983. [PubMed: 17404279]
30. Martinez-Pomares L, et al. Carbohydrate-independent recognition of collagens by the macrophage mannose receptor. *European journal of immunology.* 2006; 36:1074–1082. DOI: 10.1002/eji.200535685 [PubMed: 16619293]

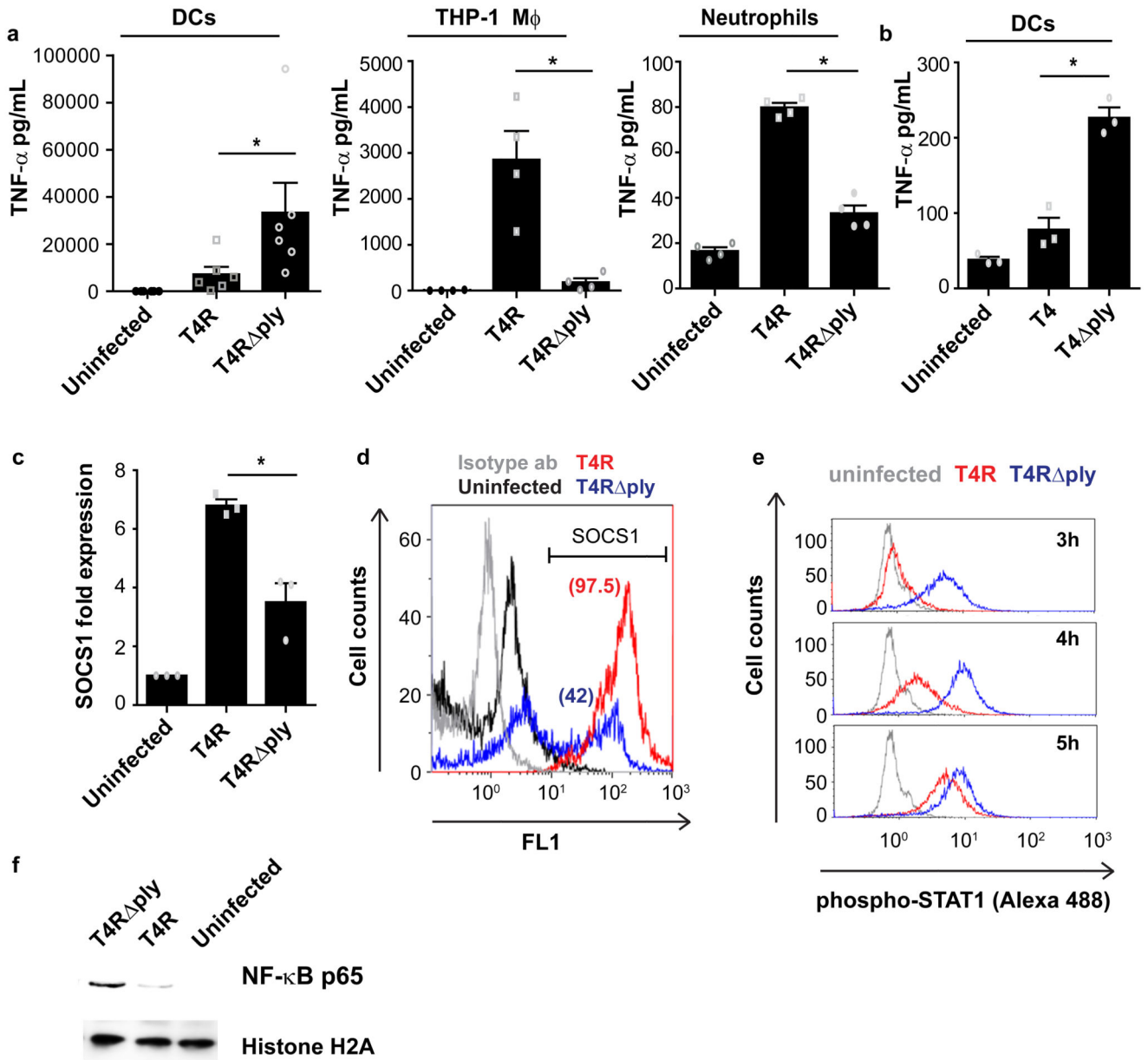


Fig. 1. Pneumolysin inhibits cytokine responses and inflammatory signalling in DCs by upregulating SOCS1.

(a) TNF- α secretion from human dendritic cells (DCs) (N=6), THP-1 macrophages (N=4), and primary neutrophils (N=4) upon infection with wild type strain T4R or its isogenic pneumolysin (PLY) mutant T4R Δ ply. Data are mean \pm SEM. *P < 0.05 by Wilcoxon matched-pairs signed (two-tailed) rank test. (b) TNF- α secretion from DCs infected with encapsulated strains, T4 or T4 Δ ply (N=3 donors). Data are mean \pm S.E.M. P < 0.05 by Wilcoxon matched-pairs signed (two-tailed) rank test. (c) SOCS1 mRNA levels in T4R or T4R Δ ply infected DCs at 9 hrs post infection (pi) (N=3 donors). Data are mean \pm S.E.M. P < 0.05 by paired two-tailed t test. (d) Flow cytometry histogram plot showing SOCS1 protein levels in T4R or in T4R Δ ply infected DCs at 9 hrs pi. Percentage of SOCS1⁺ cells is

indicated within the parenthesis. (e) STAT1 phosphorylation in T4R or in T4R *ply* infected DCs at 3-5 hrs pi. Data in d,e are representative of 3 independent experiments. (f) Western blot showing the levels of nuclear NF- κ B (p65) in T4R or T4R *ply* infected DCs at 4 hrs pi. Histone H2A served as loading controls. Blots are representative of data from 2 independent experiments.

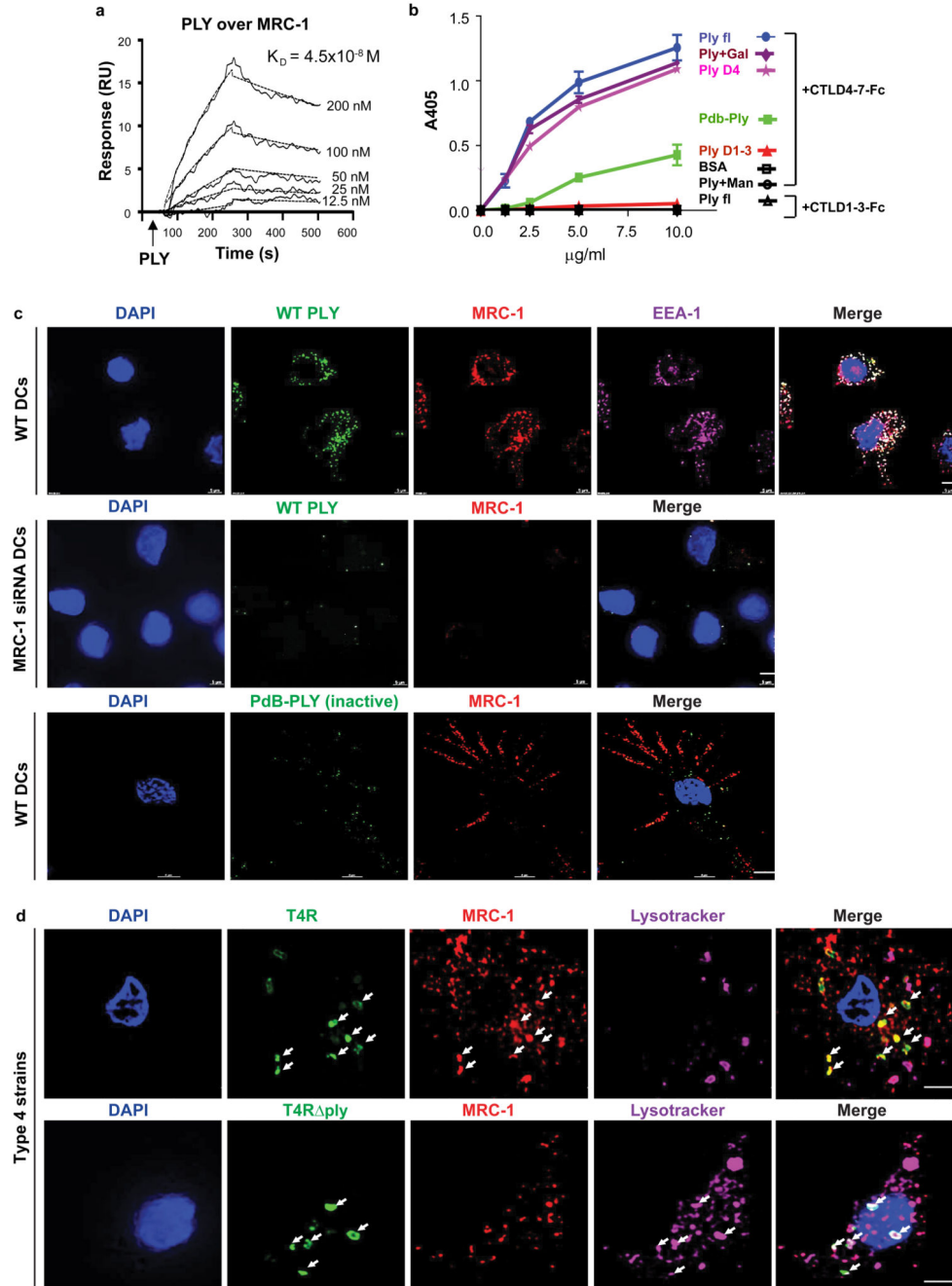


Fig. 2. MRC-1 co-localizes with pneumolysin and intracellular pneumococci in DCs. (a) Representative sensorgram of three independent surface plasmon resonance experiments showing the dose-dependent binding profile of recombinant PLY (12.5-200 nM) over immobilized MRC-1. (b) ELISA showing the binding of immobilized MRC-1 constructs, CTLD4-7-Fc or CR-FNII-CTL1-3-Fc (1.25-10 $\mu\text{g/ml}$) with full-length pneumolysin (PLY), toxoid PdB, PLY domains 1-3 and domain 4. Mannan (Man) was used as a specific ligand for CTLD4-7 to block interaction with PLY, and galactose (Gal) was used as a negative control for the blocking assay. Bound PLY was detected using anti-PLY antibodies. Data are

mean \pm S.E.M of two independent experiments, each containing 3 replicates per condition. (e) Wild type (WT) DCs or MRC-1 siRNA treated DCs were incubated with purified active PLY or mutant PLY (PdB) (200 ng/ml) for 45 min. Immunofluorescence staining show that active PLY co-localizes with MRC-1 and EEA-1 (early endosomes) in contrast to the non-pore forming mutant PLY (PdB). (d) DCs were infected with T4R or T4R *ply* for 90 min. Immunofluorescence staining showed that intracellular T4R co-localizes with MRC-1, while T4R *ply* does not co-localize with MRC-1, but with lysosomes (lysotracker) (white arrows). All scale bars, 5 μ m. Data in c,d are representative of three independent experiments.

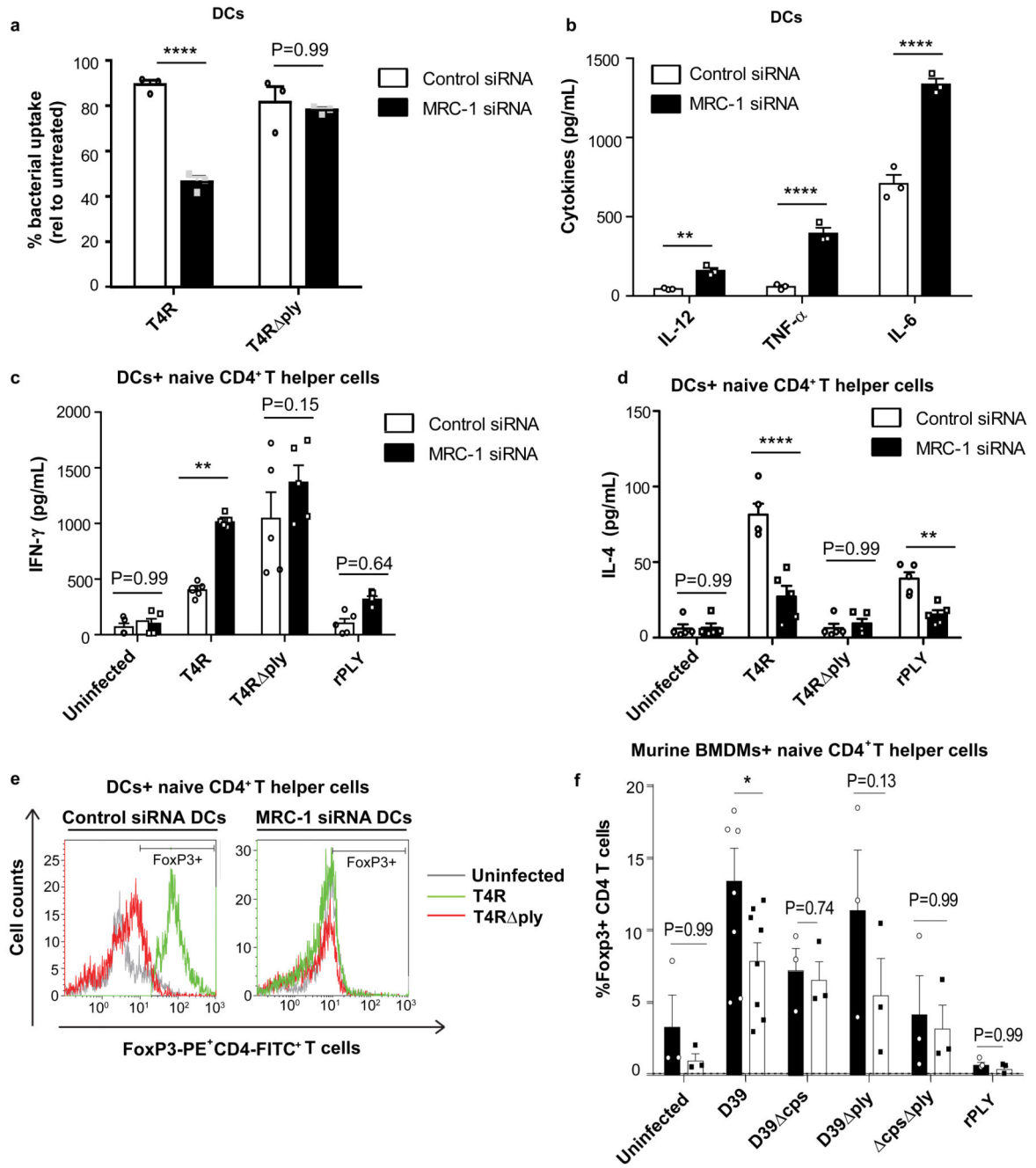


Fig. 3. Depletion of MRC-1 abolishes pneumolysin induced cytokine inhibition and enhances T cell activation.

(a) Uptake of T4R and T4R *ply* by WT and MRC-1 siRNA treated DCs (N=3 donors). The uptake was expressed as a percentage relative to untreated DCs. Data represent mean \pm S.E.M. **** denotes P<0.0001 by two-way ANOVA with Bonferroni post-test. (b) Wild type DCs (control) or MRC-1 siRNA treated DCs were infected with T4R and secretion of IL-12, TNF- α and IL-6 was measured in culture supernatants (N=3 donors). Data represent mean \pm S.E.M. **** denotes P<0.0001 and ** denotes P<0.01 by two-way ANOVA with

Bonferroni post-test. **(c-d)** Wild type or MRC-1 siRNA treated DCs were infected with T4R, T4R *ply* or recombinant PLY (rPLY) (200 ng/mL) for 24 hrs and co-cultured with naïve CD4⁺ T cells for 5 days. Secretion of **(c)** IFN- γ and **(d)** IL-4 was measured in culture supernatants (N=5 donors). Data represent mean \pm S.E.M. **** denotes P<0.0001, ** denotes P<0.01, * denotes P<0.05 by two-way ANOVA with Bonferroni post-test. **(e)** FoxP3 expression in human naïve CD4⁺ T cells upon co-culture with DCs (control or MRC-1 siRNA treated) infected with T4R or T4R *ply*. Data are representative of three independent experiments. **(f)** Percentage FoxP3⁺ CD4⁺ T cells upon co-culture with murine BMDMs (from wild type or MRC-1^{-/-} mice) that were infected with heat-killed strain D39 or mutant derivatives lacking capsule (D39 *cps*), PLY (D39 *ply*) or a double mutant (D39 *cps ply*) or purified PLY. Data represent mean \pm S.E.M. N=3, two way-ANOVA with Bonferroni multiple comparison test. * P < 0.05; **P< 0.01.

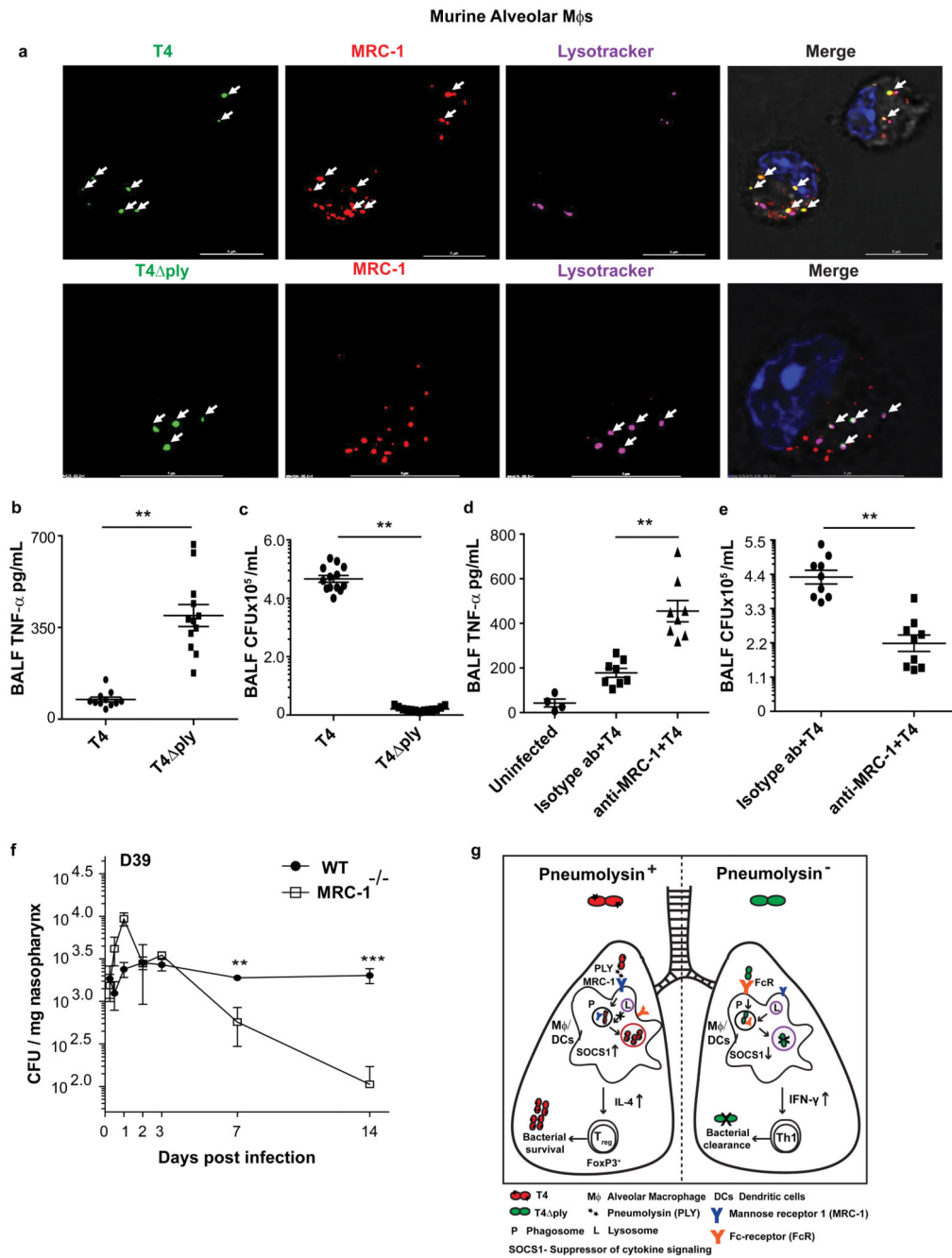


Fig. 4. MRC-1 mediates pneumolysin-induced suppression of early inflammatory responses *in vivo*.

(a) Primary alveolar macrophages were isolated from C57/BL6J mice infected with T4 or T4 *ply* at 6 hrs pi. Immunofluorescence staining showed that PLY proficient pneumococci (T4) co-localize with MRC-1 unlike T4 *ply* that co-localizes with the lysosome marker (lysotracker). Scale bars, 5 μ m. Images are representative of data from 5 mice/group. (b) TNF- α levels (N=12) and (c) bacterial count (CFU/mL) (N=13) in BALF from mice infected with either T4 or T4 *ply* at 6 hrs pi. Data are mean \pm S.E.M of three independent

experiments. ** $P < 0.01$ by Mann-Whitney (two-tailed) test. **(d)** Levels of TNF- α (N=8), and **(e)** bacterial count (CFU/mL) (N=9) in BALF of mice pretreated with anti-MRC-1 (0.1 mg/mL) or isotype antibody and infected with strain T4 for 6 hrs. Data are mean \pm S.E.M of three independent experiments. ** $P < 0.01$ by Mann-Whitney (two-tailed) test. **(f)** Bacterial count (CFU) per mg nasopharyngeal homogenates of wild type or MRC-1^{-/-} mice infected with strain D39 over a 14 day carriage experiment. N=6 mice per data point per strain, data represent mean \pm S.E.M. and analyzed by two-way ANOVA with Tukey's post-test. **(g)** Model suggested for PLY-mediated immunomodulation. PLY-proficient pneumococci induce internalization into alveolar macrophages and DCs via interaction with MRC-1. PLY-expressing pneumococci co-localize with MRC-1 in non-lysosomal compartments and block inflammatory cytokine secretion by upregulating SOCS1, thereby promoting regulatory T cell responses and bacterial survival in the airways. ** $P < 0.01$, *** $P < 0.001$.